Microbiology (2001), **147**, 2783–2794 Printed in Great Britain

Fluoranthene metabolism in *Mycobacterium* sp. strain KR20: identity of pathway intermediates during degradation and growth

Klaus Rehmann,[1,2] Norbert Hertkorn[1] and Antonius A. Kettrup[1,2]

Author for correspondence: Klaus Rehmann. Tel: +49 89 31872514. Fax: +49 89 31873372. e-mail: rehmann@gsf.de

[1] GSF – National Research Center for Environment and Health, Institute of Ecological Chemistry, Ingolstädter Landstraße 1, D-85764 Neuherberg, Germany

[2] Technical University Munich, Chair of Ecological Chemistry and Environmental Analytics, D-85350 Freising, Germany

***Mycobacterium* sp. strain KR20, which was isolated from a polycyclic aromatic hydrocarbon (PAH) contaminated soil of a former gaswork plant site, metabolized about 60% of the fluoranthene added (0·5 mg ml^{-1}) to batch cultures in mineral salts medium within 10 d at 20 °C. It thereby increased its cell number about 30-fold and produced at least seven metabolites. Five metabolites, namely *cis*-2,3-fluoranthene dihydrodiol, *Z*-9-carboxymethylene-fluorene-1-carboxylic acid, *cis*-1,9a-dihydroxy-1-hydro-fluorene-9-one-8-carboxylic acid, 4-hydroxybenzochromene-6-one-7-carboxylic acid and benzene-1,2,3-tricarboxylic acid, could be identified by NMR and MS spectroscopic techniques and ascribed to an alternative fluoranthene degradation pathway. Besides fluoranthene, the isolate could not use any of the PAHs tested as a sole source of carbon and energy.**

Keywords: biodegradation, degradation products, degradation pathway, polycyclic aromatic hydrocarbons, ring cleavage

INTRODUCTION

Polycyclic aromatic hydrocarbons (PAHs) are ubiquitous environmental contaminants, well known for their mutagenic and carcinogenic properties (Edwards, 1983; Harvey, 1991; Suess, 1976). Soil areas heavily contaminated by these compounds, such as former carbonizing plant or gasworks sites, need a proper clean-up prior to future human use and thus are major targets for the application of microbiological remediation techniques (Thomas & Lester, 1993, 1994).

During the last 15 years it has become evident that PAHs with more than three rings, despite their low water solubility, may serve as growth substrates for a number of soil bacteria. However, our knowledge of microbial transformation capabilities for PAHs with more than three rings is still limited (Kanaly & Harayama, 2000; Sutherland *et al*., 1995). The utilization of fluoranthene as a sole source of carbon and energy by a pure bacterial strain was first described by Weißenfels *et al*. (1990) and Mueller *et al*. (1990). Despite the description of several other fluoranthene-utilizing strains (Boldrin *et al*., 1993; Bouchez *et al*., 1995; Bryniok, 1994; Dagher *et al*., 1997; Ho *et al*., 2000; Juhasz *et al*., 1997; Kästner *et al*., 1994; Kleespies *et al*., 1996; Lloyd-Jones & Hunter, 1997; Mueller *et al*., 1997; Sepic *et al*., 1998; Thibault *et al*., 1996; Walter *et al*., 1991; Willumsen *et al*., 1998), data on initial metabolites are relatively scarce.

In this study we investigated the fluoranthene-degrading capability of *Mycobacterium* sp. strain KR20 (Rehmann *et al*., 1999), presenting information on the time course of fluoranthene degradation as well as detailed structural data of several metabolites. We discuss the implication of our results with respect to our current understanding of the bacterial degradation of fluoranthene, focussing on the degradation pathways known to date.

Abbreviations: COSY, correlated spectroscopy; HMBC, heteronuclear multiple bond correlation; HMQC, heteronuclear multiple quantum correlation; LC, liquid chromatography; MSTFA, *N*-methyl-*N*-(trimethylsilyl) trifluoroacetamide; NOESY, nuclear Overhauser and exchange spectroscopy; PAH, polycyclic aromatic hydrocarbon; TMS, trimethylsilyl; UV-Vis, UV–visible.

METHODS

Chemicals. Inorganic chemicals and solvents (analytical and chromatography grades, respectively) were purchased from Merck. Organic chemicals of the highest purity available were from Aldrich. Difco Bactoagar was obtained from BD GmbH, and *N*-methyl-*N*-(trimethylsilyl) trifluoroacetamide (MSTFA) used for GC-MS derivatization was from Macherey-Nagel.

Isolation and characterization of the organism. A fluoranthene-degrading mixed culture was enriched from a PAH-contaminated soil (former gasworks site, Kassel, Germany)

using a mineral salts medium (MSM) (Weißenfels *et al.*, 1990) with fluoranthene added as the sole source of carbon and energy (see below). A suspected fluoranthene-utilizing member of this bacterial community was identified by its ability to produce clear zones on fluoranthene-coated MSM agar plates (Kiyohara *et al.*, 1982) and isolated by conventional microbial techniques. It was preliminarily characterized by Gram and acid-fast staining. The mycolic acid pattern of the isolate was determined using the TLC method of Minnikin *et al.* (1975). Utilization of PAHs other than fluoranthene and of Tween 80 was studied in liquid media containing 0·5 mg ml^{-1} of the respective substrate and inoculated with MSM-washed KR20 cells pre-grown in R2A medium (Reasoner & Geldreich, 1985). R2A agar plates (20 ml) used in colony-forming units (c.f.u.) plate-counting experiments were incubated at 25 °C.

Cultivation of *Mycobacterium* sp. strain KR20. Standard cultivation conditions were as described by Rehmann *et al.* (1998) in the presence of a nominal concentration of 0·5 mg fluoranthene ml^{-1}. All cultures were incubated on a rotary shaker at 20 °C and 100 r.p.m. The optical density of 10 ml cultures was determined at 578 nm using a UVICAM 5675 spectrophotometer by means of tube-connected cuvettes (diameter 10 mm), which were mounted onto the screw caps of the culture vessels. Starter cultures (10 ml) were inoculated from R2A agar slants. After reaching an OD_{578} of 0·3–0·5 these cultures served as an inoculant (10 %, v/v) for new 10 ml or 100 ml cultures. Medium-term maintenance of the strain (up to 3 months) was performed on R2A agar slants which, after confluent growth had appeared, were stored at 4 °C, whereas −80 °C deep-frozen suspensions of R2A-agar grown cells in 50 % (w/v) glycerol were used for long-term storage.

Chromatographic analysis, preparation and identification of fluoranthene metabolites. Sample preparation for quantitative HPLC analysis was performed as described by Rehmann *et al.* (1998). Ethyl acetate extracts prepared from acidified (pH 1·5, 1 M HCl) 10 ml whole cultures were dried over anhydrous Na_2SO_4. The solvent was removed under reduced pressure and the residues dissolved in a suitable volume of methanol. Samples were analysed by HPLC (HP1090, Hewlett Packard) applying UV-Vis diode array detection and using a Baker Widebore RP18 column (J. T. Baker Inc.) at 40 °C. Fluoranthene determination was performed isocratically using a methanol/8 mM phosphoric acid 85:15 (v/v) mixture at a flow of 0·8 ml min^{-1}, applying a detection wavelength of 235 nm. Metabolite separation was achieved in a linear 8 mM phosphoric acid/methanol gradient: 0 % to 100 % methanol within 30 min at a flow of 0·8 ml min^{-1}. Metabolites were detected at 235 nm and 254 nm. UV-Vis spectra were recorded at the peak maxima and were corrected for solvent background. The recovery of fluoranthene under the extraction conditions described was > 85 % down to a concentration of 5 μg ml^{-1}.

For the purification of metabolites, eight samples of 5- to 8-d-old 100 ml cultures were filtered through glass wool to remove residual fluoranthene crystals. Combined filtrates were extracted three times with 250 ml ethyl acetate to separate excess fluoranthene and non-dissociating metabolites. The filtrates (aqueous phases) were subsequently acidified (pH 1·5, 1 M HCl) and subjected to a second threefold ethyl acetate extraction. Corresponding extracts were pooled, dried over anhydrous Na_2SO_4 and the solvent was removed under reduced pressure at 35 °C. Extraction residues dissolved in a suitable volume of methanol were fractionated by liquid chromatography (LC) (Merck-Hitachi: pump L6200, autosampler AS2000A, UV-Vis detector L4000, Merck) at room temperature on an RP18 column (250 × 10 mm, Merck Lichroprep, Merck). Selected mixtures (composition depending on the respective metabolite) of methanol and acetic acid (4 %, v/v), followed by pure methanol, served to separate the constituents of the acidic extract at a flow of 2 ml min^{-1}. For the purification of the constituents of the neutral extract, acetic acid was replaced by water. Fractions were collected according to the UV-absorbance profile of the eluates at 235 nm or 254 nm. The solvent was removed (see above) and the metabolites were redissolved in methanol. Metabolite I was further purified by TLC on silica gel plates ($60F_{254}$, 200 × 200 mm, thickness 0·25 mm, Merck) in an ethyl acetate/methanol 8:2 solvent system. The purity of the metabolites was routinely checked by HPLC and was finally ⩾ 90 %.

^{1}H- and 2D-NMR spectra were recorded with a Bruker DMX 500 spectrometer using Bruker standard software (Bruker Analytik; proton frequency 500·13 MHz) employing 2·0 mm capillaries and an inverse-geometry TXI 2·5 mm probehead (90°: 9·4 μs ^{1}H; 10·0 μs ^{13}C) in methanol-d_4, acetone-d_6 and chloroform-d_1, respectively, at 30 °C (^{1}H/^{13}C: 3·30/49·00, 2·04/29·00 and 7·24/77·00 p.p.m.). ^{1}H,^{13}C-HMBC (heteronuclear multiple bond correlation) spectra to determine the position of carbons without directly bonded protons were recorded in the absolute-value mode F1: 6800 Hz, using coupling constants of 10 Hz (metabolites I, IV), and 5, 7·5, 10 and 15 Hz (metabolite III). ^{1}H,^{13}C-HMQC (heteronuclear multiple quantum correlation) spectra to assign carbons bearing a proton were acquired by use of BIRD (bilinear rotation decoupling) pulses and ^{13}C-GARP (globally optimized alternating-phase rectangular pulses) decoupling [BIRD: 500 ms, GARP: 70 μs, aq: 95–320 ms, sw (F2): 5400 Hz, d1: 1·5–2·5 s, ^1J(CH): 145 Hz (metabolite II), 160 Hz (metabolites I, III, IV), number of increments in F1: 60–256]. The ^{13}C-NMR spectra were recorded with a 2·5 mm dual probehead (90°: 9·0 μs) with broad-band decoupling and an acquisition time of 1·0–1·9 s (relaxation delay d1: 3·5–5 s).

Absolute-value DQ-^{1}H,^{1}H-COSY (double-quantum ^{1}H,^{1}H-correlated spectroscopy) spectra (aq: 200 ms) were acquired on a Bruker AC 400 NMR spectrometer (Bruker Analytik, proton frequency: 400·13 MHz) using an inverse-geometry 5 mm probehead (90°: 8·0 μs). Phase-sensitive TPPI (time-proportional phase increment) ^{1}H,^{1}H-NOESY (nuclear Overhauser and exchange spectroscopy) spectra were recorded on the same instrument with mixing times of 800 ms (metabolites III, V) and 650 ms (metabolite IV). COSY and NOESY spectra served to establish the succession of protons in metabolites II, III, IV and V.

For GC-MS (capillary column gas chromatography-mass spectrometry) analysis, trimethylsilyl (TMS) derivatives of the metabolites were prepared according to Zink & Lorber (1995). The analysis was performed in the EI mode (70 eV) on an HP 5890 series II chromatograph (Hewlett Packard) equipped with a DB5 capillary column, 0·25 mm inside diameter by 60 m, coating 0·1 μm, coupled to a Finnigan Mat SSQ 7000 quadrupole spectrometer (Finnigan MAT GmbH). Samples were injected into the GC at 90 °C, held isothermally for 1 min, programmed to 270 °C at 15 °C min^{-1}, and held isothermally for another 20 min. A similar method was successfully applied for the analysis of bacterial fluoranthene metabolites by Sepic *et al.* (1998) and Sepic & Leskovsek (1999).

Direct-infusion LC-MS was performed on a Perkin Elmer Sciex API 300 LC-MS/MS system (Perkin Elmer Überlingen).

Samples were dissolved in water/methanol (1:1, v/v) and injected into the mass spectrometer via a syringe pump (Harvard Apparatus) at a flow of 5 μl min^{-1}. Ionization was achieved in the negative mode with the ion spray interface set at −3·5 kV. Nitrogen was used as nebulizer gas (1·5 l min^{-1}) and curtain gas (1·2 l min^{-1}). Lens and quadrupole parameters were set as follows: orifice −30 V, focusing ring −200 V, Q0 10 V. All other parameters were optimized with regard to signal intensity. LC2 Tune 1.2 and Multiview 1.2 software (Perkin Elmer Sciex) were used for data acquisition and evaluation.

RESULTS

Characterization of the fluoranthene-degrading isolate strain KR20

Strain KR20 (Rehmann *et al*., 1999) was isolated from a PAH-contaminated soil by its ability to utilize fluoranthene as sole source of carbon and energy. The rod-shaped (diameter 0·5–0·8 μm, length 1·5–2 μm), Gram-negative, non-motile bacterium produced smooth, yellow, scotochromogenic colonies of 2–3 mm diameter on R2A agar plates after 7 d at 25 °C. Due to its pronounced acid-fastness, its mycolic acid pattern, which was similar to that of *Mycobacterium phleii* DSM 43239, and its ability to utilize Tween 80, another taxonomic characteristic (Wayne *et al*., 1974), isolate KR20 was assigned to the genus *Mycobacterium*. For growth on fluoranthene (10 ml batch cultures, 0·5 mg fluoranthene ml^{-1}) a linear relationship between the turbidity (OD_{578}) of the cultures and the number of c.f.u. was observed in the range of OD_{578} 0·03–0·5 ($r^2 = 0{\cdot}952$), resulting in $1{\cdot}56 \times 10^8$ cells ml^{-1} at an OD_{578} of 0·1.

Although metabolites were produced from several other PAHs (Table 1) none of these compounds was able to support the growth of strain KR20, i.e. they failed to increase the number of c.f.u. over a 14 d incubation period.

Fluoranthene metabolites

Structures of known bacterial fluoranthene degradation intermediates and the corresponding degradation pathways are summarized in Fig. 1. Seven metabolites were produced by strain KR20 from fluoranthene in detectable amounts. They could be differentiated into three neutral and four acidic compounds by sequential neutral and acidic ethyl acetate extraction of the cultures (Rehmann *et al*., 1999). Comparison of the UV-Vis spectra of the metabolites with those of known PAH metabolites gave a first indication of the identity of the compounds.

Metabolite I had no UV-Vis absorption maximum above 220 nm (Fig. 2). Its ^{1}H-NMR spectrum (Table 2), showing only two signals in the aromatic region with a 2/1 intensity ratio, indicated a 1,2,3-symmetrically substituted benzene skeleton. The corresponding ^{13}C-NMR data (Table 2) revealed six signals, two of which showed a chemical shift characteristic of carboxy carbon atoms. In accordance with the symmetry requirements imposed by the ^{1}H-NMR signature, the investigation of ^3J(CH) coupling (Table 2) indicated that the six signals observed in the ^{13}C-NMR spectrum were caused by nine carbon atoms, the actual number of carboxy substituents being three. The correct assignment of the resulting structure benzene-1,2,3-tricarboxylic acid (hemimellitic acid) was checked by MS techniques. Metabolite I could not be derivatized with MSTFA for GC-MS analysis; however, direct-infusion HPLC-negative-mode MS derived mass spectra showed the expected M−H signal at m/z 209. Fragment ions were observed at m/z 191 (M−H−H_2O), 165 (M−H−CO_2), 147 (M−H−CO_2−H_2O) and 121 (BP;

Table 1. Metabolism of substrates other than fluoranthene by *Mycobacterium* sp. strain KR20 cells after 14 d incubation

Substrate (0·5 mg ml^{-1})	Metabolites	
	*n**	Structure proposal†
None	–	–
Biphenyl	–	–
Naphthalene	1	–
Anthracene	2	1,2-Anthracene dihydrodiol
Fluorene	1	9-Hydroxyfluorene
Phenanthrene	3	Diphenic acid, 3-hydroxyphenanthrene
Pyrene	4	4,5-Pyrene dihydrodiol, 4,5-phenanthrene dicarboxylic acid, pyrene metabolite VI‡
Chrysene	–	–

* *n*, number of metabolites detected

† Preliminary structure assignments are based on UV-Vis spectral data as obtained by diode-array detection during HPLC analysis of ethyl acetate extracts of the acidified cultures (HPLC conditions same as for fluoranthene metabolite separation).

‡ See Rehmann *et al*. (1999).

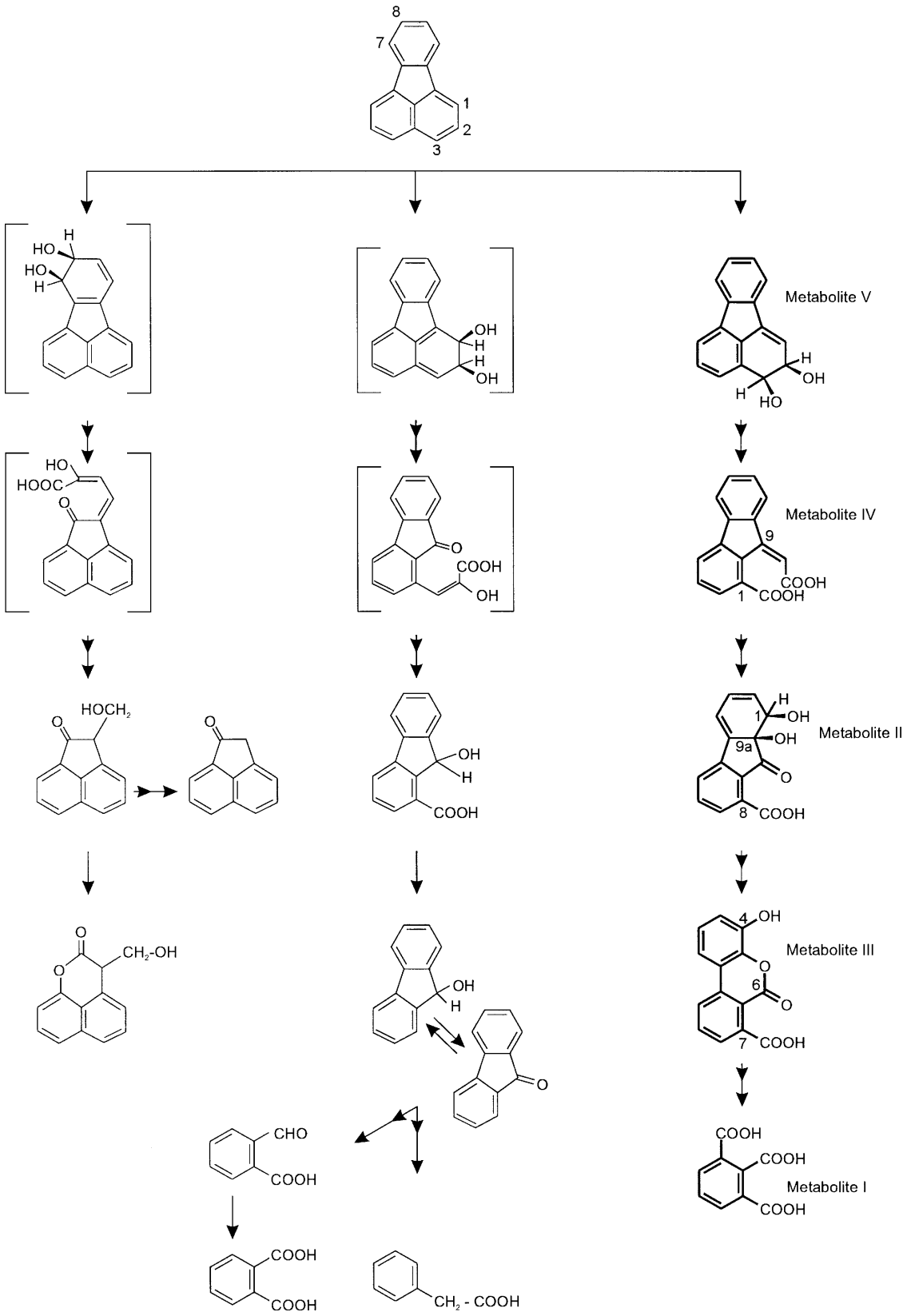

Fig. 1. Synopsis of bacterial fluoranthene degradation pathways described to date: left column, Weißenfels *et al.* (1990); middle column, Kelley *et al.* (1993); right column, Rehmann *et al.* (1999). Single arrows indicate one-step reactions, double arrows transformations of two or more steps. Hypothetical intermediates are shown in square brackets. Ring numbering follows IUPAC rules; cf. Tables 2–6.

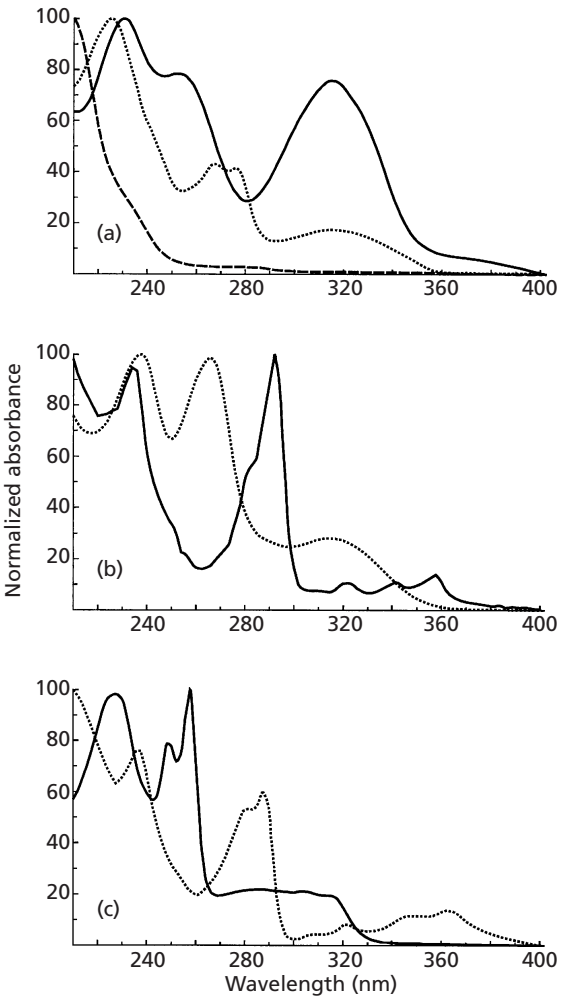

Fig. 2. UV-Vis spectra of fluoranthene metabolites I–VII of *Mycobacterium* sp. strain KR20 as obtained during HPLC analysis of ethyl acetate culture extracts by diode-array detection, corrected for solvent background. (a) ---, Metabolite I; ——, metabolite II; · · ·, metabolite III. (b) · · ·, Metabolite IV; ——, metabolite VI, (c) · · ·, Metabolite VII; ——, metabolite V.

$M-H-2CO_2$). The structure was finally confirmed by co-chromatographic HPLC analysis and direct-infusion HPLC-MS comparison of authentic hemimellitic acid.

The UV-Vis spectrum of metabolite II (Fig. 2) was very similar to the UV-Vis spectrum of *cis*-1,9a-dihydroxy-1-hydrofluoren-9-one (Grifoll *et al*., 1994). The ^{1}H-NMR data (Table 3) also revealed a striking similarity to the ^{1}H-NMR spectrum of this compound (Selifonov *et al*., 1993), the only difference being a substituted carbon atom in ring position 8. The ^{13}C-NMR spectrum (Table 3) showed an insufficient signal/noise ratio due to the limited amount of material available. Additional weak quaternary carbon atom signals were observed at 133·3, 134·7, 144·4 and 147·8 p.p.m., with two further signals missing which were expected from the structure. The signals could not unequivocally be assigned to the non-hydrogen-bearing carbon atoms at ring positions 4a, 4b, 8, 8a, 9, and 9a. However, the substituent at ring position 8 could be identified from the ^{13}C-NMR spectrum as carboxylic acid methyl ester. From the increased HPLC retention time observed for the purified compound (15·2 min) as compared to metabolite II in culture extracts (13·2 min), it was concluded that metabolite II artificially recruited the methoxy group during purification due to the concentration process of the acidified methanolic clean-up fractions. Thus native metabolite II was assigned the structure *cis*-1,9a-dihydroxy-1-hydrofluoren-9-one-8-carboxylic acid. GC-MS analysis of the trimethylsilylated derivative of metabolite II methyl ester confirmed this assignment. As expected the molecule ion signal was observed at m/z 416 (BP, 100%). Characteristic fragment ions were detected at m/z 401 (18·6%, M^+-CH_3), 385 (8·8%, M^+-OCH_3, ester group), 369 (16·2%, $M^+-CH_3OH-CH_3$), 327 (14·9%, M^+-OTMS), 311 (73·5%, M^+-HOTMS $-CH_3$), 297 (10·3%, M^+-OTMS$-2CH_3$), 269 (11·2%) and 223 (84·2%, M^+-2OTMS$-CH_3$).

Comparison of the UV-Vis spectra of metabolite III (Fig. 2) and of 4-hydroxy-benzo[c]chromene-6-one [designated by Grifoll *et al*. (1994) as 8-hydroxy-3,4-benzocoumarin] indicated a high degree of concurrence. The same held for the NMR characteristics of both compounds. Metabolite III differed in only one position: the ring carbon atom on position 7 of the 4-hydroxy-benzo[c]chromene-6-one skeleton. By ^{13}C-NMR measurements (Table 4) this carbon atom was shown to carry a carboxy group. The unequivocal signal assignment in ^{1}H-NMR and ^{13}C-NMR spectra was carried out by a combination of HMQC and HMBC spectra. The deduced structure of metabolite III, 4-hydroxy-benzo[c]chromene-6-one-7-carboxylic acid, was further confirmed by GC-MS analysis of the MSTFA-derivatized compound. Its mass spectrum, which showed the expected M^+ signal at m/z 400 (22·7%), gave only a poor fragmentation pattern with fragment ions observed at m/z 385 (BP, 100%, M^+-CH_3), 311 (7·8%, M^+-OTMS), 240 (3·9%, M^+-TMS$-$COOH$-$CO$-CH_3$) and 210 (4·2%, M^+-2HOTMS).

The ^{1}H-NMR data of metabolite IV (Table 5) revealed the presence of three mutually coupling groups encompassing one methylene proton, and four and three aromatic protons, respectively. The succession of the protons as deduced from ^{1}H,^{1}H-COSY and ^{1}H,^{1}H-NOESY experiments suggested that the basic molecular frame was a fluorene substituted at ring positions 1 and 9, the latter resulting from a ring opening between the carbon atoms 2 and 3 of the parent compound fluoranthene. The ^{13}C-NMR signature of metabolite IV (Table 5) encompassed 14 signals, only seven of which showed directly bound protons as demonstrated by a DEPT 135 (distortionless enhancement by polarization transfer) experiment. A ^{1}H,^{13}C-HMQC spectrum revealed that the signal observed at 130·95 p.p.m. was actually caused by two carbon atoms occupying ring

Table 2. NMR data of fluoranthene metabolite I, benzene-1,2,3-tricarboxylic acid, hemimellitic acid (methanol-d_4, 30 °C)

r, ring atom position.

^{13}C-NMR						
Structural assignments	r1/r3	r2	r4/r6	r5	at r1/r3	at r2
Chemical shift (p.p.m.)	130·85	138·63	134·94	130·09	168·46	172·82
^1J(CH)			+	+	carboxylate	
^3J(CH) to proton at	r5	r4			r4	
^{1}H-NMR						
Structural assignments			at r4/r6	at r5		
Chemical shift (p.p.m.)*			8·17	7·61		
Signal intensity			2	1		
Signal multiplicity			d	t		
^3J coupling constants (Hz)			7·8	7·9		

* The signals of the carboxylate protons were invisible due to chemical exchange.

Table 3. NMR data of fluoranthene metabolite II, *cis*-1,9a-dihydroxy-1-hydrofluoren-9-one-8-carboxylic acid methyl ester (chloroform-d_1, 30 °C)

r, ring atom position.

^{13}C-NMR*									
Structural assignments	r1	r2	r3	r4	r5†	r6	r7†	at r8	OCH_3
Chemical shift (p.p.m.)	70·73	133·58	123·72	118·92	135·37	129·82	124·64	166·69	52·78
^1J(CH)	+	+	+	+	+	+	+	carboxy	+
^{1}H-NMR									
Structural assignments	at r1	at r2	at r3	at r4	at r5	at r6	at r7		at OCH_3
Chemical shift (p.p.m.)‡	4·73	5·96	6·22	6·63	7·68	7·70	7·84		3·97
Signal intensity	1	1	1	1	1	1	1		3
Signal multiplicity	d	dd	ddd	d	dd	dd	dd		s
^3J coupling constants (Hz)	2·0	2·0	9·6	5·1	7·4	7·5	7·5		
		9·6	5·1			7·5			

* Additional weak quaternary carbon atom signals were observed at 133·3, 134·7 144·4 and 147·8 p.p.m. These signals could not unequivocally be assigned.

† Deduced by comparison with the ^{1}H-NMR data published for *cis*-1,9a-dihydroxy-1-hydrofluoren-9-one (Selifonov *et al*., 1993).

‡ The signals of exchangeable protons were invisible due to traces of water in the sample.

positions 3 and 6 in the supposed fluorene scaffold. The remaining seven ^{13}C signals could be subdivided into six sp^2-hybridized carbon atoms and one carboxylic carbon atom. A ^{1}H,^{13}C-HMBC experiment, performed to establish the assignment of the non-hydrogen substituted carbon resonances, revealed the presence of a second carboxy group (Table 5) bound to the carbon at ring position 1. Metabolite IV was assigned the structure of *Z*-9-carboxymethylenefluorene-1-carboxylic acid. The *Z*-configuration of the carboxy and fluorene 'substituents' of the methylene group was deduced from the ^{1}H,^{1}H-NOE (nuclear Overhauser effect) observed with the methylene proton and the proton at ring carbon atom on position 8. The mass spectrum obtained from the trimethylsilylated derivative of metabolite IV was in accordance with the structure proposed, providing an M^+ signal at m/z 410 (10·3 %). Fragmentation was even poorer than that observed with metabolite III. Signals were detected at m/z 395 (8·8 %, $M^+ - CH_3$), 293 (BP, 100 %, $M^+ - TMS - CO_2$,), 235 (2·3 %, $M^+ - 2TMS - CHO$), 190 (2·1 % $M^+ - 2TMS - CO_2 - CH_2O$) and 176 (3·1 %, $M^+ - 2TMS - 2CO_2$).

Metabolite V had a UV-Vis spectrum (Fig. 2) almost identical to that of *trans*-2,3-fluoranthene dihydrodiol as published by Babson *et al*. (1986) and Pothuluri *et al*. (1992). The assignment of the fluoranthene dihydrodiol structure was confirmed by the results of the GC-MS analysis of the MSTFA-derivatized compound. The mass spectrum showed the expected M^+ signal at m/z 380 (BP, 100 %). Prominent fragment ions were detected at m/z 365 (3·9 %, $M^+ - CH_3$), 349 (6·3 %, $M^+ - CH_3O$), 291 (27·3 %, $M^+ - OTMS$), 290 (25·7 %, $M^+ - HOTMS$), 275 (12·3 %, $M^+ - HOTMS - CH_3$),

Table 4. NMR data of fluoranthene metabolite III, 4-hydroxy-benzo[c]chromene-6-one-7-carboxylic acid (acetone-d_6, 30 °C)

r, ring atom position.

^{13}C-NMR															
Structural assignments	r1	r2	r3	r4	r4a	r5	r6	r6a	r7	r8	r9	r10	r10a	r10b	at r7
Chemical shift (p.p.m.)	114·81	125·60	118·36	146·23	140·95	oxygen atom	158·93	136·78	139·27	128·32	135·36	124·41	118·15	119·25	169·98
^1J(CH)	+	+	+				lactone			+	+	+			carboxy
$^n J$(CH) to proton at*				r3**	r2****		r10****	r9****	r9***				r10**	r2***	r8***
^{1}H-NMR															
Structural assignments	at r1	at r2	at r3	at r4						at r8	at r9	at r10			
Chemical shift (p.p.m.)	7·78	7·25	7·14	8·90†						7·63	7·98	8·43			11·45§
Signal intensity	1	1	1	–‡						1	1	1			–‡
Signal multiplicity	dd	dd	dd	s						dd	dd	dd			
^3J (Hz)	8·2	8·1								7·4	7·5				
		8·0	8·0								8·1	8·3			

* The data presented are from ^{1}H,^{13}C-HMBC experiments and show the strongest interactions observed (**$n = 2$; ***$n = 3$; ****$n = 4$).

† Hydroxyl proton.

‡ Not integrated due to signal broadening.

§ Carboxylate proton.

Table 5. NMR data of fluoranthene metabolite IV, *Z*-9-carboxymethylene-fluorene-1-carboxylic acid (methanol-d_4, 30 °C)

r, ring atom position.

^{13}C-NMR																
Structural assignments	r1	r2	r3	r4	r4a	r4b	r5	r6	r7	r8	r8a	r9	r9a	at r1	10 at r9	at 10
Chemical shift (p.p.m.)*	134·39	129·65	130·95	123·40	144·84	139·89	120·88	130·95	129·06	121·80	141·12	145·65	135·42	171·76	120·15	170·47
^1J(CH)		+	+	+			+	+	+	+				carboxy	+	carboxy
$^n J$(CH) to proton at†	r3				r3/r5	r4/r6					10/r7	r8	r4/r2	r2		10††
^{1}H-NMR																
Structural assignments		at r2	at r3	at r4			at r5	at r6	at r7	at r8					at 10	
Chemical shift (p.p.m.)‡		7·71	7·51	7·91			7·76	7·43	7·34	7·80					6·89	
Signal intensity		1	1	1			1	1	1	1					1	
Signal multiplicity		dd	dd	dd			d	ddd	ddd	d					s	
^3J coupling constants (Hz)		7·7	7·7				7·5	7·5	7·4							
			7·6	7·3				7·4	7·7	7·7						

* Complete overlap of the signals of the carbon atoms assigned to positions 3 and 6 was recognized from a ^{1}H,^{13}C-HMQC experiment. The signal of the carboxy group connected to ring position 1 was detected with a ^{1}H,^{13}C-HMBC-experiment.

† The data presented are from ^{1}H,^{13}C-HMBC experiments and show the strongest interactions observed ($n = 3$, ††$n = 2$).

‡ The signals of the carboxylate protons were invisible due to chemical exchange.

Table 6. ^{1}H-NMR data of fluoranthene metabolite V, *cis*-2,3-fluoranthene dihydrodiol (*acetone-d_6*, 30 °C)

r, ring atom position

Structural assignments	r1	r2	r3	r4	r5	r6	r7	r8	r9	r10
Chemical shift (p.p.m.)	6·73	4·72/ 4·15*	4·88/ 4·10*	7·39	7·37	7·64	7·80	7·40	7·33	7·82
Signal intensity	1	1/–†	1/–†	1	1	1	1	1	1	1
Signal multiplicity‡	d	dd	d	d	dd	d	d	ddd	ddd	d
^3J coupling constants (Hz)§	4·1	4·1		7·2	7·3	7·2	7·5	7·5	7·5	7·5
		5·4	**5·4**		7·4			7·5	7·4	

* Hydroxyl protons.

† Hydroxyl protons not integrated due to signal broadening.

‡ After addition of H_2O to exchange the hydroxyl protons.

§ The coupling constants of the *cis*-protons are given in bold.

218 (32·5%, $M^+-TMS-OTMS$) and 202 (17·5%, $M^+-2OTMS$). The ^{1}H-NMR data of metabolite V (Table 6) again were in good accordance with those of *trans*-2,3-fluoranthene dihydrodiol (Pothuluri *et al.*, 1992; Rice *et al.*, 1983). However, the ^3J vicinal coupling constant between the protons at ring positions 2 and 3 was different: 5·4 Hz as compared to 8 Hz for *trans*-2,3-fluoranthene dihydrodiol, suggesting a *cis*-orientation of the substituents. Such smaller coupling constants of the *cis*-isomers were also reported for the 1,2-dihydrodiols of naphthalene, anthracene and phenanthrene (Jeffrey *et al.*, 1975; Jerina *et al.*, 1976).

The UV-Vis spectra of metabolites VI and VII (Fig. 2) showed a striking similarity to the UV-Vis spectra of 8-hydroxyfluoranthene and 3-hydroxyfluoranthene (Babson *et al.*, 1986) and were thus assigned these structures. They could not be characterized in more detail because their concentrations varied very markedly from experiment to experiment.

Time course of fluoranthene degradation

Fluoranthene metabolism of *Mycobacterium* sp. strain KR20 was monitored over 624 h (Fig. 3) using 10 ml batch cultures which were inoculated to an OD_{578} of 0·03 with cells pre-grown on fluoranthene for 6 d. Fluoranthene degradation started without an apparent lag and cell counts began to rise after 48 h. Maximum c.f.u. numbers (about $6{\cdot}2 \times 10^8$ cells ml^{-1}), a 30-fold increase compared to the inoculum, were obtained between day 10 and 14 of the cultivation period, when $\geqslant 60\%$ of the initial fluoranthene content was metabolized. The c.f.u. numbers decreased considerably afterwards. The fluoranthene degradation eventually reached $> 96\%$, whereas sterile controls run in parallel showed no loss of fluoranthene after 624 h.

Metabolites I to IV could be quantified from the beginning of the experiment. In contrast, metabolite V, *cis*-2,3-fluoranthene dihydrodiol, was detected only in trace amounts over the whole incubation period. Absolute concentrations could only be determined for metabolite I, as sufficient amounts for HPLC calibration of metabolites II to IV could not be obtained. Metabolite I reached a maximum concentration of 8 μg ml^{-1}, which accounted for about 0·8% of the fluoranthene carbon added. The concentrations of all metabolites increased up to day 10–14. Later on, the concentration of metabolite I increased further, whereas the concentrations of metabolites II and IV reached a plateau and the concentration of metabolite III decreased after 20 d.

The situation when non-fluoranthene-grown inocula were used was slightly different (data not shown). As indicated by the turbidity increase of these cultures, cells started to grow only after a lag phase of about 72 h. Depending on the respective experiment a temporary accumulation of *cis*-2,3-fluoranthene dihydrodiol during the first 120 h up to 192 h of incubation could be observed.

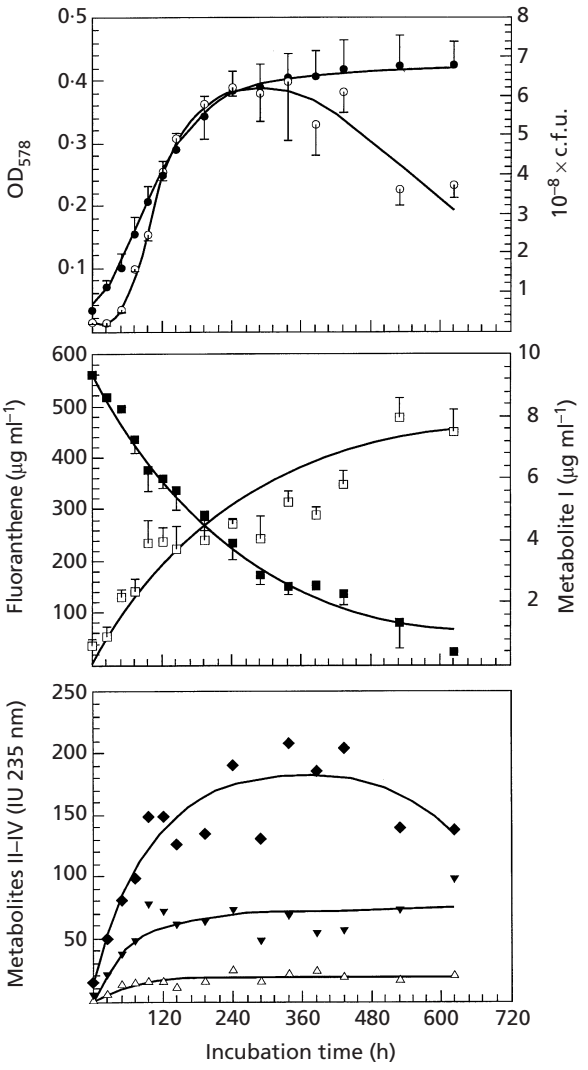

Fig. 3. Fluoranthene degradation and metabolite formation by *Mycobacterium* sp. strain KR20. The optical density values represent the mean of six 10 ml cultures; the c.f.u. numbers and concentration determinations represent the mean of three 10 ml cultures. Error bars indicate the standard deviation (plotted unidirectionally for better visibility). The inoculum was pre-grown on fluoranthene. ○, c.f.u.; ●, optical density; ■, fluoranthene; □, metabolite I; ▼, metabolite II; ◆, metabolite III; △, metabolite IV. IU, integration units of the chromatographic signals. Underlying curves are only intended to visualize the respective trends.

DISCUSSION

Fluoranthene metabolites and degradation pathways

In contrast to bacterial pyrene degradation, where only one degradative metabolic route is known to date (Rehmann *et al.*, 1998), there seem to exist at least three bacterial pathways for fluoranthene utilization (see Fig. 1). For *Alcaligenes denitrificans* Weißenfels *et al.* (1990) proposed an initial attack at the 7,8-position of the benzylic moiety of the fluoranthene skeleton (Fig. 1, left column), which after ring opening between positions 6b and 7 yields the two metabolic intermediates observed:

1-acenaphthenone and subsequently 3-hydroxymethylbenzo[d,e]chromen-2-one (designated as 7-acenaphthenone and 3-hydroxymethyl-4,5-benzocoumarin by the authors). Naphthalene-1,8-dicarboxylic acid as a fluoranthene metabolite of *Sphingomonas paucimobilis* EPA505 (formerly classified as *Pseudomonas paucimobilis*) was described by Mueller *et al*. (1990, and unpublished results), and ascribed to the metabolic pathway proposed by Weißenfels *et al*. (1990). For *Mycobacterium* sp. strain PYR1 and *Pasteurella* sp. strain IFA Kelley *et al*. (1993) and Sepic *et al*. (1998) deduced two different primary dioxygenation sites from the metabolites identified: the 7,8-position according to the former authors from the formation of 1-acenaphthenone, and the 1,2-position in the naphthoic substructure of the fluoranthene molecule due to the occurrence of 1-carboxy-9-hydroxyfluorene, 1-carboxyfluoren-9-one, 9-hydroxyfluorene and fluorene-9-one (Fig. 1 middle column). The late fluoranthene degradation products observed by these authors, namely 2-carboxybenzaldehyde, phthalic acid, phenylacetic acid, benzoic acid and adipic acid, could not be unequivocally linked to one of preceding metabolites. However, neither the *cis*-7,8-fluoranthene dihydrodiol nor the *cis*-1,2-fluoranthene dihydrodiol postulated as initial metabolites by Weißenfels *et al*. (1990), Kelley *et al*. (1993) and Sepic *et al*. (1998) have yet been detected, thus leaving a crucial gap in the proposed pathways.

The five fluoranthene metabolites identified from cultures of *Mycobacterium* sp. strain KR20 supported a degradation route (Fig. 3, right column) previously outlined by Rehmann *et al*. (1999). Fluoranthene metabolism by this isolate obviously seems to start with a dioxygenation of the fluoranthene molecule in the 2,3-position, yielding *cis*-2,3-fluoranthene dihydrodiol (metabolite V). The follow-up product expected, 2,3-dihydroxyfluoranthene, could not, however, be detected. But this also holds for the analogous *ortho*-dihydroxy PAH derivatives in the degradation pathways of anthracene (Fernley *et al*., 1964) and pyrene (Dean-Ross & Cerniglia, 1996; Heitkamp *et al*., 1988; Rehmann *et al*., 1998; Walter *et al*., 1991), probably due to a strong association of the dihydroxy metabolites with the enzymes involved in their turnover. The *ortho* ring cleavage of 2,3-dihydroxyfluoranthene leads to the formation of metabolite IV, which subsequently probably loses a C_2-unit, hypothetically producing 1-carboxyfluorene-9-one. This compound, in contrast to its successor, metabolite II, could not be detected in cultures of strain KR20.

The consequence of this hypothesis is that strain KR20, *Mycobacterium* sp. strain PYR 1 (Kelley *et al*., 1993) and *Pasteurella* sp. IFA (Sepic *et al*., 1998) might use homologous entry reactions for fluoranthene degradation, implying that the initial dioxygenation by the latter strains also takes place in the 2,3-position. However, the final aromatic metabolites identified by Kelley *et al*. (1993) and Sepic *et al*. (1998) suggest a divergence of the metabolic routes in a later stage of degradation, i.e. the breakdown of the fluorene scaffold. Metabolite II in turn represents the substrate for the second ring-opening reaction, which might proceed by two alternative mechanisms: either by a dehydrogenation of the secondary hydroxy group at C-1 resulting in the formation of a spontaneously hydrolysing 1,3-diketone whose hydrolysis product under acidic conditions (as prevailing during metabolite clean-up) should easily dehydrate to yield the corresponding δ-lactone (Grifoll *et al*., 1994), or by a biological Baeyer–Villiger reaction as suggested for the fluoranthene degradation pathway proposed by Weißenfels *et al*. (1990). However, the resulting product, metabolite III, after hydrolysis is most likely metabolized analogously to biphenyl (Higson, 1992), since the formation of metabolite I (hemimellitic acid), which represented the last detectable aromatic intermediate, requires the opening of the hydroxylated ring of metabolite III in a biphenyl-like manner. The fate of metabolite I is unclear at the moment and warrants further investigation.

This fluoranthene degradation pathway seems also to be operative in *Mycobacterium hodleri* inasmuch as Kleespies *et al*. (1996) reported *cis*-2,3-fluoranthene dihydrodiol as the only identifiable metabolite (without any structural proof) and the UV-Vis spectra of two other fluoranthene metabolites of this isolate were identical to the UV-Vis spectra of *Mycobacterium* sp. KR20 metabolites III and IV, respectively (H. Kneifel, personal communication).

The degradative route outlined closely corresponds to a fluorene degradation pathway discovered in a *Pseudomonas* sp. by Grifoll *et al*. (1994). Starting with the second dihydrodiol metabolite (metabolite II) of the fluoranthene degradation pathway of strain KR20, characterized intermediates of both pathways are homologues: metabolite II versus *cis*-1,9a-dihydroxy-1-hydrofluorene-9-one, metabolite III versus 4-hydroxybenzo[c]chromene-6-one, and metabolite I versus phthalic acid. The fluoranthene descendants differ from their respective fluorene counterparts each by one additional carboxy group in one of the aromatic rings. This homology might point to an evolutionary relation between the two sets of degradative enzymes, but, as already mentioned, strain KR20 was not able to utilize fluorene as a growth substrate. The reason for the latter observation might be based on the requirement of the dioxygenase involved in the formation of the angular dihydrodiol of an activated carbon atom on position 9 as given when attacking fluoren-9-one (Bressler & Fedorak, 2000). However, this hypothesis still has to be investigated.

The fact that isolate KR20 did not produce any fluoranthene metabolite attributable to the 'acenaphthenone' route of fluoranthene degradation present in the strains investigated by Kelley *et al*. (1993), Sepic *et al*. (1998), Weißenfels *et al*. (1990) and J. G. Mueller, S. E. Lantz & C. E. Cerniglia (unpublished results) in our opinion might be related to the inability of *Mycobacterium* sp. strain KR20 to use any other PAH as growth substrate, but this question also requires more detailed investigations.

Table 7. Utilization of PAH as sole growth substrates by currently known fluoranthene-utilizing (bold) and fluoranthene-degrading bacteria

Isolate	PAH as sole growth substrate*:						Reference
	NAP	ANT	PHE	FLU	PYR	CRY	
NOCARDIOFORMS							
***Mycobacterium* sp. KR20**	−	−	−	−	−	−	This work
***Mycobacterium gilvum* BB1**	o	o	+	−	+	o	Boldrin *et al.* (1993); Böttger *et al.* (1997)
***Mycobacterium* sp. PY**	o	o	+	o	+	o	Bryniok (1994)
***Mycobacterium* sp. PY18**	o	o	+	o	+	o	Bryniok (1994)
Mycobacterium flavescens	o	o	+	−	+	o	Dean-Ross & Cerniglia (1996)
Mycobacterium austroafricanum PYR-1	+	+	+	o	+	o	Kelley *et al.* (1993); Böttger *et al.* (1997)
***Mycobacterium* sp. VF1**	+	+	+	o	+	−	Kästner *et al.* (1994)
Mycobacterium hodleri	o	−	−	−	−	o	Kleespies *et al.* (1996); Böttger *et al.* (1997)
***Mycobacterium* sp. G4**	o	o	+	+	+	o	Lloyd-Jones & Hunter (1997)
***Mycobacterium* sp. O1**	o	o	−	−	−	o	Lloyd-Jones & Hunter (1997)
***Mycobacterium* sp. Fan9**	o	o	o	o	o	o	Willumsen *et al.* (1998)
***Rhodococcus* sp. SPyrNa1**	o	o	+	−	+	o	Bouchez *et al.* (1995)
***Rhodococcus* sp. SFltNa1**	o	o	+	−	+	o	Bouchez *et al.* (1995)
***Rhodococcus* sp. UW1**	o	+	+	−	+	+	Walter *et al.* (1991)
***Gordona* sp. BP9**	+	−	+	o	+	−	Kästner *et al.* (1994)
Coryneform SAntMu3	o	+	+	−	+	o	Bouchez *et al.* (1995)
NON-NOCARDIOFORMS							
***Pseudomonas* sp. K12**	+	+	+	o	+	o	Thibault *et al.* (1996)
***Pseudomonas putida* Ph61**	o	o	+	o	+	o	Bryniok (1994)
***Pseudomonas aeruginosa* AK1**	o	o	+	o	+	o	Bryniok (1994)
***Sphingomonas paucimobilis* EPA505†**	+	+	+	−	−	−	Mueller *et al.* (1990)
***Sphingomonas* sp. FLA 1-1‡**	o	o	+	o	o	o	Ho *et al.* (2000)
***Sphingomonas* sp. FLA 4-1‡**	o	o	−	o	o	o	Ho *et al.* (2000)
***Sphingomonas* sp. FLA 6-1‡**	o	o	+	o	o	o	Ho *et al.* (2000)
***Sphingomonas* sp. CO6‡**	o	o	+	+	o	o	Ho *et al.* (2000)
***Sphingomonas yanoikuyae* 107**	o	o	o	o	+	o	Dagher *et al.* (1997)
***Xanthomonas maltophilia* N3F2§**	o	o	o	o	o	o	Mueller *et al.* (1997)
***Pasteurella* sp. IFA**	o	o	o	o	o	o	Sepic *et al.* (1998)
Burkholderia cepacia VUN 10001‖	o	o	+	+	+	o	Juhasz *et al.* (1997)
***Alcaligenes denitrificans* WW1**	+	+	+	−	−	−	Weißenfels *et al.* (1990)

* Abbreviations: NAP, naphthalene; ANT, anthracene; PHE, phenanthrene; FLU, fluorene; PYR, pyrene; CRY, chrysene. Symbols: +, growth; −, no growth; o, no data published.

† Originally classified as *Pseudomonas paucimobilis* EPA505.

‡ Representatively selected from a total of 27 Gram-negative fluoranthene degraders described with 11 strains identified as *Sphingomonas* sp.

§ Eight fluoranthene degraders were isolated; only one gave conclusive results in classification.

‖ One out of three very similar strains described.

Time course of fluoranthene degradation

Strain KR20 pre-grown on fluoranthene degraded the same compound in batch cultures without any apparent lag phase, thereby increasing its cell number about 30-fold within 10–14 d and excreting limited amounts of the metabolites reported above. As mentioned, the situation with non-fluoranthene-grown inocula was different. The temporary accumulation of *cis*-2,3-fluoranthene dihydrodiol observed in this case might be caused by an induction event, i.e. the dihydrodiol accumulated only until the degradation pathway enzymes were fully induced. A comparable transient accumulation of primary dihydrodiol metabolites was reported for the degradation of phenanthrene and pyrene by *Mycobacterium* sp. strain KR2 (Rehmann *et al.*, 1996, 1998).

Since under any conditions, none of the metabolites accumulated in a 1:1 stoichiometric ratio to the amount of fluoranthene added, it may be assumed that no real dead-end metabolites (in the sense of being not substrates for any degradative enzyme of the strain) were produced. Rather, the amount of degradation products

found might be interpreted as spillover of the cells due to the large amount of growth substrate available or compounds which cannot be reassimilated, e.g. due to their ionic character.

Fluoranthene-degrading bacteria

Mycobacterium sp. strain KR20 represents one of about 50 bacterial fluoranthene degraders described during recent years (Table 7). Currently the number of Gram-negative isolates, especially *Sphingomonas* sp., matches or even outnumbers the number of Gram-positive fluoranthene-utilizing bacteria (Mueller *et al*., 1997; Ho *et al*., 2000). This finding is in contrast to the situation with pyrene-degrading bacteria, where nocardioforms (Gram-positives) constitute the majority of species described so far (Ho *et al*., 2000; Kästner *et al*., 1994; Rehmann *et al*., 1998), a fact that was ascribed to the facilitated interaction of hydrophobic PAH with the outer cell surface of Gram-positive bacteria, which is also hydrophobic in nature (Rehmann *et al*., 1998). However, it is still open to discussion (Mueller *et al*., 1997) to what extent the enrichment techniques used bias the ratio depicted in Table 7. For example, Bastiaens *et al*. (2000) demonstrated that the type of fluoranthene degrader isolated from the same soil sample was clearly dependent on the kind of enrichment technique applied, whereas Mueller *et al*. (1997), in several cases, obtained similar spectra of fluoranthene-degrading organisms despite applying different kinds of enrichment procedures to the same soil sample.

Another interesting aspect arising from Table 7 is that the fluoranthene degraders seem to form two clusters with respect to their PAH-utilization capabilities. One set, containing most of the organisms studied, encompasses strains capable of utilizing at least two or more of the three- and four-ring PAHs as a sole source of carbon and energy (which appears to be quite common among PAH-degrading bacteria). In contrast, the members of the second set, *Mycobacterium* sp. strain KR20 (Rehmann *et al*., 1999; this work), *Mycobacterium hodleri* (Kleespies *et al*., 1996), *Mycobacterium* sp. strain O1 (Lloyd-Jones & Hunter, 1997) and *Sphingomonas* sp. strain FLA 6-1 (Ho *et al*., 2000) appear to be unable to use any other PAH besides fluoranthene as a sole growth substrate. Restrictions concerning the PAH-utilization pattern of bacteria were also observed by other authors but seemed to be associated with the bacterial type (Gram-positive or Gram-negative) or genera investigated (Ho *et al*., 2000; Kästner *et al*., 1994; Mueller *et al*., 1997). The reason for the substrate specificity of these Gram-positive and Gram-negative strains deserves further investigation.

ACKNOWLEDGEMENTS

We wish to thank Mr A. Papaderos for the preparative clean-up of some of the metabolites, Ms L. Lattmann and Mr S. Achatz for performing the GC-MS and HPLC-MS measurements, respectively, and Dr. J. G. Mueller (Dames & Moore, Chicago, USA) and Professor H. Kneifel (ICG 6, Forschungszentrum Jülich) for additional information and helpful discussions.

REFERENCES

Babson, J. R., Russo-Rodruiguez, S. E., Wattley, R. V., Bergstein, P. L., Rastetter, W. H., Liber, H. L., Andon, B. M., Thilly, W. G. & Wogan, G. N. (1986). Microsomal activation of fluoranthene to mutagenic metabolites. *Toxicol Appl Pharm* **85**, 355–366.

Bastiaens, L., Springael, D., Wattiau, P., Harms, H., deWachter, R., Verachtert, H. & Diels, L. (2000). Isolation of adherent polycyclic aromatic hydrocarbon (PAH)-degrading bacteria using PAH-sorbing carriers. *Appl Environ Microbiol* **66**, 1834–1843.

Boldrin, B., Thiem, A. & Fritsche, C. (1993). Degradation of phenanthrene, fluorene, fluoranthene, and pyrene by a *Mycobacterium* sp. *Appl Environ Microbiol* **59**, 1927–1930.

Böttger, E. C., Kirschner, P., Springer, B. & Zumft, W. (1997). Mycobacteria degrading polycyclic aromatic hydrocarbons. *Int J Syst Bacteriol* **47**, 247.

Bouchez, M., Blanchet, D. & Vandecasteele, J.-P. (1995). Degradation of polycyclic aromatic hydrocarbons by pure strains and by defined strain associations: inhibition phenomena and cometabolism. *Appl Microbiol Biotechnol* **43**, 156–164.

Bressler, D. C. & Fedorak, P. M. (2000). Bacterial metabolism of fluorene, dibenzofurane, dibenzothiophene, and carbazole. *Can J Microbiol* **46**, 397–403.

Bryniok, D. (1994). PAK-Abbau in Mehrphasensystemen. In *Biologischer Abbau von polycyclischen aromatischen Kohlenwasserstoffen*, pp. 91–108. Edited by B. Weigert. Berlin: SFB 193 der TU Berlin.

Dagher, F., Deziel, E., Lirette, P., Paquette, G., Bisaillon, J.-G. & Villemur, R. (1997). Comparative study of five polycyclic aromatic hydrocarbon degrading bacterial strains isolated from contaminated soils. *Can J Microbiol* **46**, 368–377.

Dean-Ross, D. & Cerniglia, C. E. (1996). Degradation of pyrene by *Mycobacterium flavescens*. *Appl Microbiol Biotechnol* **46**, 307–312.

Edwards, N. T. (1983). Polycyclic aromatic hydrocarbons (PAH's) in the terrestial environment – a review. *J Environ Qual* **12**, 427–441.

Fernley, H. N., Griffiths, E. & Evans, W. C. (1964). Oxidative metabolism of phenanthrene and anthracene by soil bacteria: the initial ring-fission step. *Biochem J* **91**, 15p-16p.

Grifoll, M., Selifonov, S. A. & Chapman, P. J. (1994). Evidence for a novel pathway in the degradation of fluorene by *Pseudomonas* sp. strain F274. *Appl Environ Microbiol* **60**, 2438–2449.

Harvey, R. G. (1991). *Polycyclic Aromatic Hydrocarbons: Chemistry and Carcinogenicity*. New York, Port Chester, Melbourne, Sydney: Cambridge University Press.

Heitkamp, M. A., Franklin, W. & Cerniglia, C. E. (1988). Microbial metabolism of polycyclic aromatic hydrocarbons: isolation and characterization of a pyrene-degrading bacterium. *Appl Environ Microbiol* **54**, 2549–2555.

Higson, F. (1992). Microbial degradation of biphenyl and its derivatives. *Adv Appl Microbiol* **37**, 135–164.

Ho, Y., Jackson, M., Yang, Y., Mueller, J. G. & Pritchard, P. H. (2000). Characterization of fluoranthene- and pyrene-degrading bacteria isolated from PAH-contaminated soils and sediments. *J Ind Microbiol Biotechnol* **24**, 100–112.

Jeffrey, A. M., Yeh, H. J. C., Jerina, D. M., Patel, T. R., Davey, J. F. & Gibson, D. T. (1975). Initial reactions in the oxidation of naphthalene by *Pseudomonas putida*. *Biochemistry* **14**, 575–584.

Jerina, D. M., Selander, H., Yagi, H., Wells, M. C., Davey, J. F., Mahadevan, V. & Gibson, D. T. (1976). Dihydrodiols from anthracene and phenanthrene. *J Am Chem Soc* **98**, 5988–5996.

Juhasz, A. L., Britz, M. L. & Stanley, G. A. (1997). Degradation of fluoranthene, pyrene, benz[a]anthracene and dibenz[a,h]anthracene by *Burkholderia cepacia*. *J Appl Microbiol* **83**, 189–198.

Kanaly, R. A. & Harayama, S. (2000). Biodegradation of high-molecular-weight polycyclic aromatic hydrocarbons by bacteria. *J Bacteriol* **182**, 2059–2067.

Kästner, M., Breuer-Jammali, M. & Mahro, B. (1994). Enumeration and characterization of the soil microflora from hydrocarbon-contaminated soil sites able to mineralize polycyclic aromatic hydrocarbons (PAH). *Appl Microbiol Biotechnol* **41**, 267–273.

Kelley, I., Freeman, J., Evans, F. E. & Cerniglia, C. E. (1993). Identification of metabolites from the degradation of fluoranthene by *Mycobacterium* sp. strain PYR-1. *Appl Environ Microbiol* **59**, 800–806.

Kiyohara, H., Nagao, K. & Yana, K. (1982). Rapid screen for bacteria degrading water-insoluble, solid hydrocarbons on agar plates. *Appl Environ Microbiol* **43**, 454–457.

Kleespies, M., Kroppenstedt, R. M., Rainey, F. A., Webb, L. E. & Stackebrandt, E. (1996). *Mycobacterium hodleri*, sp. nov., a new member of the fast-growing mycobacteria capable of degrading polycyclic aromatic hydrocarbons. *Int J Syst Bacteriol* **46**, 683–687.

Lloyd-Jones, G. & Hunter, D. W. F. (1997). Characterization of fluoranthene- and pyrene-degrading *Mycobacterium*-like strains by RAPD and SSU sequencing. *FEMS Microbiol Lett* **153**, 51–56.

Minnikin, D. E., Alshamaony, L. & Goodfellow, M. (1975). Differentiation of *Mycobacterium*, *Nocardia*, and related taxa by thin-layer chromatographic analysis of whole-organism methanolysates. *J Gen Microbiol* **88**, 200–204.

Mueller, J. G., Chapman, P. J., Blattmann, B. O. & Pritchard, P. H. (1990). Isolation and characterization of a fluoranthene-utilizing strain of *Pseudomonas paucimobilis*. *Appl Environ Microbiol* **56**, 1079–1086.

Mueller, J. G., Devereux, R., Santavy, D. L., Lantz, S. E., Willis, S. G. & Pritchard, P. H. (1997). Phylogenetic and physiological comparison of PAH-degrading bacteria from geographically diverse soils. *Antonie Leeuwenhoek* **71**, 329–343.

Pothuluri, J. V., Heflich, R. H., Fu, P. P. & Cerniglia, C. E. (1992). Fungal metabolism and detoxification of fluoranthene. *Appl Environ Microbiol* **58**, 937–941.

Reasoner, D. J. & Geldreich, E. E. (1985). A new medium for the enumeration and subculture of bacteria from potable water. *Appl Environ Microbiol* **49**, 1–7.

Rehmann, K., Steinberg, C. E. W. & Kettrup, A. A. (1996). Branched metabolic pathway for phenanthrene degradation in a pyrene-degrading bacterium. *Polycycl Aromat Comp* **11**, 125–130.

Rehmann, K., Noll, H. P., Steinberg, C. E. W. & Kettrup, A. A. (1998). Pyrene degradation by *Mycobacterium sp*. strain KR2. *Chemosphere* **36**, 2977–2992.

Rehmann, K., Hertkorn, N. & Kettrup, A. A. (1999). Bacterial fluoranthene degradation – indication for a novel degradation pathway. In *Novel Approaches for Bioremediation of Organic Pollution; Proceedings of the 42nd Oholo Conference Eilat, Israel* (3.5–7.5.1998), pp. 39–46. Edited by R. Fass, Y. Flashner & S. Reuveny. New York, Boston, Dordrecht, London, Moscow: Kluwer Academic/Plenum.

Rice, J. E., LaVoie, E. J. & Hoffmann, D. (1983). Synthesis of the isomeric phenols and the *trans*-2,3-dihydrodiol of fluoranthene. *J Org Chem* **48**, 2360–2363.

Selifonov, S. A., Grifoll, M., Gurst, J. E. & Chapman, P. J. (1993). Isolation and characterization of (+)-1,1a-dihydroxy-1-hydroxyfluoren-9-one formed by angular dioxygenation in the bacterial catabolism of fluorene. *Biochem Biophys Res Commun* **193**, 67–76.

Sepic, E. & Leskovsek, H. (1999). Isolation and identification of fluoranthene biodegradation products. *Analyst* **124**, 1765–1769.

Sepic, E., Bricelj, M. & Leskovsek, H. (1998). Degradation of fluoranthene by *Pasteurella* sp. IFA and *Mycobacterium* sp. PYR1: isolation and identification of metabolites. *J Appl Microbiol* **85**, 746–754.

Suess, M. J. (1976). The environmental load and cycle of polycyclic aromatic hydrocarbons. *Sci Total Environ* **6**, 239–250.

Sutherland, J. B., Rafii, F., Khan, A. A. & Cerniglia, C. E. (1995). Mechanisms of polycyclic aromatic hydrocarbon degradation. In *Microbial Transformation and Degradation of Toxic Organic Chemicals*, pp. 269–306. Edited by L. Y. Young & C. E. Cerniglia. New York, Chichester, Brisbane, Toronto, Singapore: Wiley-Liss.

Thibault, S. L., Anderson, M. & Frankenberger, W. T., Jr (1996). Influence of surfactants on pyrene desorption and degradation in soils. *Appl Environ Microbiol* **61**, 283–287.

Thomas, A. O. & Lester, J. N. (1993). The microbial remediation of former gasworks sites: a review. *Environ Technol* **14**, 1–24.

Thomas, A. O. & Lester, J. N. (1994). The reclamation of disused gaswork sites: new solutions to an old problem. *Sci Total Environ* **152**, 239–260.

Walter, U., Beyer, M., Klein, J. & Rehm, H.-J. (1991). Degradation of pyrene by *Rhodococcus* sp. UW1. *Appl Microbiol Biotechnol* **34**, 671–676.

Wayne, L. G., Engbœk, C., Engel, H. B. W. & 17 other authors (1974). Highly reproducible techniques for use in systematic bacteriology in the genus *Mycobacterium*: tests for pigment, urease, resistance to sodium chloride, hydrolysis of Tween 80, and β-galactosidase. *Int J Syst Bacteriol* **24**, 412–419.

Weißenfels, W. D., Beyer, M. & Klein, J. (1990). Degradation of phenanthrene, fluorene and fluoranthene by pure bacterial cultures. *Appl Microbiol Biotechnol* **32**, 479–484.

Willumsen, P. A., Karlson, U. & Prichard, P. H. (1998). Response of fluoranthene-degrading bacteria to surfactants. *Appl Microbiol Biotechnol* **50**, 475–483.

Zink, G. & Lorber, K. E. (1995). Mass spectral identification of metabolites formed by microbial degradation of polycyclic aromatic hydrocarbons (PAH). *Chemosphere* **31**, 4077–4084.

Received 2 March 2001; revised 30 May 2001; accepted 8 June 2001.